Synthesis, Structure, DNA binding, cleavage and biological activity of Cobalt (III) complexes derived from Triethylenetetramine and 1,10 phenanthroline ligands

ARTICLE *in* INORGANICA CHIMICA ACTA · MAY 2014

Impact Factor: 2.05 · DOI: 10.1016/j.ica.2014.03.015

3 AUTHORS, INCLUDING:

Harikesavan Gopinathan
Independent Researcher
7 PUBLICATIONS **4** CITATIONS
SEE PROFILE

M.N. Arumugham
Thiruvalluvar University
31 PUBLICATIONS **178** CITATIONS
SEE PROFILE

Inorganica Chimica Acta 416 (2014) 93–101

Contents lists available at ScienceDirect

Inorganica Chimica Acta

journal homepage: www.elsevier.com/locate/ica

Synthesis, structure, DNA binding, cleavage and biological activity of cobalt (III) complexes derived from triethylenetetramine and 1,10 phenanthroline ligands

H. Gopinathan [a], N. Komathi [b], M.N. Arumugham [a,*]

[a] Department of Chemistry, Thiruvalluvar University, Serkadu, Vellore 632 115, Tamil Nadu, India
[b] Department of Chemistry, Muthurangam Govt. Arts College, Vellore 632 002, Tamil Nadu, India

ARTICLE INFO

Article history:
Received 28 December 2013
Received in revised form 6 March 2014
Accepted 11 March 2014
Available online 26 March 2014

Keywords:
Triethylenetetramine
Crystal structure
DNA binding
Groove binding
Cytotoxic activity
Antimicrobial activity

ABSTRACT

The cobalt (III) complexes, [Co(trien)(phen)] $(ClO_4)_2Cl$, (**1**), [Co(trien)(phen)]$(NO_3)_3$, (**2**) (where trien = triethylenetetramine, phen = 1,10-phenanthroline) has been synthesized and characterized by Infra-red, UV–Vis, ESI-MS and elemental analysis methods. Complex **1** was structurally characterized by single crystal X-ray crystallography. It was crystallized in a triclinic system with space group $P\bar{1}$, $a = 7.797(10)$ Å, $b = 10.6584(2)$ Å, $c = 14.889(3)$ Å, $\alpha = 96.83(10)°$, $\beta = 96.16(10)°$, and $\gamma = 98.88(10)°$. The cobalt atom assumes a distorted octahedral geometry by coordinating to 6 nitrogen atoms from four triethylenetetramine and two 1,10-phenanthroline ligands. The binding of this cobalt (III) complex with calf thymus DNA (CT-DNA) was investigated by UV–Vis absorption, fluorescence spectroscopic, cyclic voltammetric and viscosity techniques. Also, the interactions of pBR322 DNA with these cobalt (III) complexes were studied using the gel electrophoresis method. The thermal denaturation and viscosity binding data advocates that the cobalt (III) complexes interact with DNA by groove binding. When compared to complex **2** complex **1** has more potential to the kill human liver cancer cell as revealed by the MTT assay. The cobalt (III) complexes screened for their activities *in vitro* on common bacteria and fungi and exhibit antimicrobial activities.

1. Introduction

The deoxyribonucleic acid (DNA) plays an important role in the life process, because it delivers inheritance information and instructs the biological synthesis in living cells. DNA particularly offers a wide variety of potential metal binding sites [1–4]. Such sites include the electron rich DNA bases or phosphate groups that are available for direct covalent coordination to the metal and they occur: (i) between two base pairs (intercalation), (ii) in the minor groove, (iii) in the major groove, and (iv) on the outside of the helix [5,6].

The interaction of transition metal complexes with DNA has long been a subject of intensive investigation with the perspective of development of newer materials for application in biotechnology and medicine [7,8]. The effect of size, shape, hydrophobicity, and the charge on the binding of the complex to DNA has been studied by changing the type of hetero aromatic ligand or metal center [9,10]. Cobalt is documented as metal widely distributed in the biological system such as cells and body, and the interaction of cobalt complex with DNA has attracted much attention [11–14]. Besides, the DNA binding studies, cobalt complexes have been investigated for their anticancer properties [15,16]. Cobalt (III) complexes have also been tested as hypoxia-activated anticancer prodrugs which upon reduction in the reducing environment of cancer tissues could release toxic ligands to kill the cancer cells [17].

In this paper, we report two Co (III) complexes with trien and phen, ligands and different counter anions. The syntheses, characterization, DNA binding and cleavage abilities of two cobalt (III) complexes [Co(trien)(phen)]$(ClO_4)_2Cl$ **1** and [Co(trien)(phen)]$(NO_3)_3$ **2**. Complex **1** was structurally characterized by single crystal X-ray crystallography is reported. The DNA binding of cobalt (III) complexes were examined by absorption spectroscopy, fluorescence spectroscopy, cyclic voltammetry and viscosity measurements. The result should be of value in further understanding the binding modes of the complexes to DNA. Their ability to induce the cleavage of pBR322 DNA also investigated. The cytotoxic activity of complexes **1** and **2** against human liver cancer cell Hep-G_2 and antimicrobial activities of the two cobalt (III) complexes

* Corresponding author. Tel.: +91 416 2704053; fax: +91 416 2407043.
E-mail address: aru_mugham@yahoo.com (M.N. Arumugham).

http://dx.doi.org/10.1016/j.ica.2014.03.015
0020-1693/

against certain human pathogenic microorganisms are also reported.

2. Methods

2.1. Synthesis of cobalt (III) complexes

The complex $[Co(trien)Cl_2]Cl$ was synthesized according to the procedure outlined by Sargeson and Searle [18].

2.1.1. Synthesis of $[Co\ (trien)(phen)]\ (ClO_4)_2Cl$

1.5622 g (5 mmol) of $[Co(trien)Cl_2]Cl$ complex was dissolved in equal ratio of 1:1 (25 ml) ethanol and water was added to that and stirred well. About 0.9912 g (5 mmol) of 1,10 phenanthroline was dissolved in 25 ml of ethanol. Then this solution was added to the above solution the mixture was refluxed for 5 h in the water bath. On cooling the solution to ambient temperature, an aqueous solution of sodium perchlorate 12.244 g (10 mmol) was added to the above mixture and then refluxed for 30 min. The filtrate on slow evaporation gave single crystal suitable for X-ray diffraction. The red crystal was isolated and washed with aqueous ethanol (1:1 v/v) before drying over P_4O_{10} (Yield: ~74%). *Anal.* Calc. for $C_{18}H_{26}Cl_3CoN_6O_8$: C, 34.89; H, 4.23; N, 13.56. Found: C, 34.76; H, 4.18; N, 13.45%. IR/cm^{-1} (KBr): 3446br, 3246w, 3075br, 1618m, 1524w, 1438s, 1093vs, 847m, 780w, 720m, 624s cm^{-1}, M.P. 290 °C. Λ_o ($Sm^2\ mol^{-1}$) in water at 25 °C: 389.

Caution! Although no problems were encountered in this work, perchlorate salts of transition metal complexes with organic ligands are potential explosives. Only small amount of material should be prepared and handled with caution.

2.1.2. Synthesis of $[Co(trien)(phen)](NO_3)_3$

1.5622 g (5 mmol) of $[Co(trien)Cl_2]Cl$ complex was dissolved in equal ratio of 1:1 (25 ml) ethanol and water added to that and stirred well. About 0.9912 g (5 mmol) of 1,10 phenanthroline was dissolved in 25 ml of ethanol. Then this was added to the above solution the mixture was refluxed for 5 h in the water bath. On cooling the solution to ambient temperature, an aqueous solution of 4.5495 g (15 mmol) of potassium nitrate was added then refluxed for 30 min. The filtrate on slow evaporation red colored crystalline product was obtained (Yield: ~69%). *Anal.* Calc. for $C_{18}H_{26}CoN_9O_9$: C, 37.84; H, 4.59; N, 22.06. Found: C, 37.17; H, 4.38; N, 22.02%. IR/cm^{-1} (KBr): 3432br, 3095br, 1632s, 1531m, 1443s, 1381vs, 1352w, 1223m, 1145m, 1053m, 847s, 789m, 719s cm^{-1}. M.P. 297 °C. Λ_o ($Sm^2\ mol^{-1}$) in water at 25 °C: 395.

2.2. DNA-binding and cleavage experiments

2.2.1. Abssorption spectroscopic studies

The DNA-binding experiments were performed at 30 ± 0.2 °C. The DNA concentration per nucleotide was determined by electronic absorption spectroscopy (UV–Vis–NIR Cary300 spectrophotometer) using cuvettes of 1 cm path length. Solutions of DNA in buffer of 50 mM NaCl and 5 mM Tris–HCl in water, gave the ratio of UV absorbance at 260 and 280 nm, A_{260}/A_{280}, of 1.9, indicating that the DNA was sufficiently free of protein [19]. The concentration of DNA in nucleotide phosphate was determined by UV absorbance at 260 nm after 1:100 dilutions by taking the extinction coefficient λ_{260} nm as 6600 $M^{-1}\ cm^{-1}$ [20]. Absorption titration experiments of cobalt (III) complex in buffer (50 mM NaCl-5 mM Tris–HCl, pH 7.1) were performed by using a fixed complex concentration to which increments of the DNA stock solutions were added. Cobalt (III) complex-DNA solutions were allowed to incubate for 10 min before the absorption spectra were recorded.

2.2.2. Fluorescence binding study

For fluorescence quenching experiments DNA was pretreated with ethidium bromide for 30 min. The cobalt (III) complexes were then added to this mixture and their effect on the emission intensity was measured using Jobin Yvon Fluorolog-3 spectroflurimeter. Samples were excited at 450 nm and emission was observed between 500 and 700 nm.

2.2.3. Thermal denaturation studies

The thermal denaturation studies were performed on Perkin-Elmer Lambda 35 spectrophotometer equipped with a Peltier temperature-controlling programmer (PTP 6) (±0.1 °C) on increasing the temperature of the solution by 1 °C per min. CT DNA (60 μM) was treated with **1** and **2** (60 μM) in a 1:1 ratio in buffer (5 mM Tris–HCl/50 mM NaCl) at pH 7.5. The samples were continuously heated at the rate of 1 °C min^{-1} temperature increase, while the absorption changes at 260 nm were monitored. Values for melting temperature (T_m) and for the melting interval (ΔT_m) were determined according to the reported procedures [21].

2.2.4. Viscosity measurement

Viscosity experiments were carried out using an Ostwald viscometer maintained at a constant temperature of 25.0 ± 0.1 °C in a thermostatic water bath, each sample was measured three times and an average flow time was calculated. Calf thymus DNA samples, approximately 200 base pairs in average length, were prepared by soliciting in order to minimize complexities arising from DNA flexibility [22]. Data were presented as $(\eta/\eta_0)^{1/3}$ versus binding ratio [23], where η is the viscosity of DNA in the presence of Co (III) complex and η_o is the viscosity of DNA alone. The relative viscosity was calculated according to the relation $\eta = (t - t_o)/t_o$, Where, t_o is the flow time for the buffer and t is the observed flow time for DNA in the presence and absence of the complex [24].

2.2.5. Cyclic voltammetry

Cyclic Voltammetry (CV) was performed on a CHI 600 C series electrochemical analyzer by a three electrode system. The three electrode system consisted of a glassy carbon (GC) electrode as the working electrode, saturated calomel electrode (SHE) as the reference electrode and Pt wire as the counter electrode. Supporting electrolytes were Tris buffer (pH 7.2). Before each experiment, the supporting electrolytes were deaerated via purging pure N_2 for 15 min and nitrogen atmosphere was kept over the solution during the experiments.

2.2.6. DNA cleavage study

For the gel electrophoresis experiments, super coiled pBR322 DNA (0.11 g) was treated with the cobalt (III) complex in 50 mM Tris–HCl, 18 mM NaCl buffer, (pH 7.2). The samples were subjected to electrophorese for 3 h at 50 V on a 0.8% agarose gel in Tris–acetic acid-EDTA buffer. The gel was stained with 0.5 l μg/mL of ethidium bromide and photographed under UV light using Chemi smart 3000 image illuminator (Vilber-lourmat, France). The extent of DNA cleavage was quantified via fluoro imaging. Control experiments were carried out using $[Co(H_2O)_6]Cl_2$, free ligands (1,10-phenanthroline mono hydrate and triethylenetetramine) at 1 mM. To know the involvement of free radicals (hydroxyl radical) in oxidative and hydrolytic DNA cleavage, experiments were also carried out by adding radical scavenger (DMSO, 25 mM) to complex-DNA mixture.

2.3. Microbial assay

The *in vitro* antimicrobial screening of the cobalt (III) complexes were tested for its effect on both the Gram +ve (*Staphylococcus aureus*, *Bacillus subtilis*) and Gram −ve (*Escherichia coli*, *Pseudomonas*

aeruginosa) bacteria and Candida albicans by disc diffusion method. The complex was stored at dry room temperature and dissolved in DMSO. The bacteria were grown in nutrient agar medium and incubated at 37 °C for 48 h followed by frequent subculture to fresh medium and was used in this test. *Candida albicans* were grown in Sabourad's dextrose agar medium were incubated at 27 °C for 72 h followed by periodic sub-culturing in fresh medium and were used in this test. The petriplates were inoculated with a loopful of bacterial or fungal culture and was spread uniformly throughout the petriplates with a sterile glass spreader. On this culture, paper discs were placed and to each disc the test samples dissolved in water at a concentration of 1 μg% was added while Ciprofloxacin (1 μg/disc for bacteria) and Clotrimazole (10 μg/disc for fungus) were used as reference antimicrobial agent. The plates were then incubated at 35 ± 2 °C for 48 h and 27 ± 1 °C for bacteria and fungus, respectively. Plates with disc containing respective solvents served as control. Inhibition was recorded by measuring the diameter of the inhibitory zone after the period of incubation.

2.4. Cell culture

Hep-G2 human liver cancer cell and Dox normal cells were cultured as a monolayer supplemented with 10% fetal bovine serum (FBS) and 100 μg/mL of streptomycin as antibiotic (Himedia, Mumbai, India), in 96 well culture plates, at 37 °C, in a humidified atmosphere of 5% CO_2, inside a CO_2 incubator (Heraeus, Hanau, Germany). All experiments were performed using cells from passage 15 or less.

2.4.1. MTT assay

The *in vitro* cytotoxicity of complexes **1** and **2** were investigated. The $HepG_2$ cells were plated separately in 96 well plates at a concentration of 1×10^5 cells/well. After 24 h, cells were washed twice with 100 μl of serum-free medium and starved for an hour at 37 °C. After starvation, cells were treated with different concentrations of test compound (25–200 μg/ml) for 24 h. At the end of the treatment period the medium was aspirated and serum free medium containing MTT (0.5 mg/ml) was added and incubated for 4 h at 37 °C in a CO_2 incubator. The 50% inhibitory concentration values (IC_{50}) of the complexes were detected. At the end of incubation period, the MTT containing medium was then discarded and the cells were washed with PBS (200 μl). The complexes were then dissolved by adding 100 μl of DMSO and this was mixed properly by pipetting up and down. Spectrophotometrical absorbance of the purple blue formazan dye was measured in a microplate reader at 570 nm (Biorad 680). Cytotoxicity was determined using Graph pad prism5 software. The growth inhibitory rate of treated cells was calculated by $(OD_{control}–OD_{test})/OD_{control} \times 100\%$. Detailed experimental procedures are similar to those reported previously [25].

2.4.2. DNA fragmentation analysis

For the DNA fragmentation assay, HepG2 cells were treated with complexes **1** and **2**. The DNA concentration and quality were analysed by electrophoresis. The complexes were applied to a 1.5% agarose gel and subjected to electrophoresis for 2 h at 80 V with running buffer of TAE. The gel was stained, destained, and photographed under UV light using a Syngene Bio Imaging system and the digital image was viewed with Gene Flash software.

2.5. X-ray crystallography

X-ray diffraction study was carried out using a Bruker kappa Apex II Single crystal difractometer equipped with Mo Kα ($\lambda = 0.7107$ Å) radiation. A blocky red crystal of size $0.2 \times 0.2 \times 0.15$ mm^3 was cut and mounted on a glass fiber using cyanoacrylate. The unit cell parameters were determined from 36 frames measured from three different crystallographic zones and using the method of difference vectors. Indexing for cell parameters show that the compound was crystallized in triclinic system with space group $P\bar{1}$. The collected intensity data frames were integrated, Lorentz-Polarization correction and decay correction were done using SAINT-(APEX-II) software [26]. Empirical absorption correction (multi-scan) was performed using SADABS program [27]. The structure was solved by direct methods using SIR92 [28] followed by the refinement by full-matrix least squares refinement on F^2 using SHELXTL-97 program [29]. All the non-hydrogen atoms were refined anisotropically. All the hydrogen atoms could be located in the difference Fourier map. Selected crystallographic data are summarized in Table 1. The CCDC deposition number of the crystal is 922741.

3. Results and discussion

3.1. Synthesis and characterization

The cobalt (III) complexes synthesized in the present study were characterized by UV–Vis, ESI-Mass and IR spectroscopy. The purity of the complexes was checked by elemental analyses, which were in good agreement with the calculated values. Conductance measurement revealed [30,31] that the cobalt (III) complexes **1** and **2** behave as 1:3 electrolyte in aqueous medium. The ESI-MS spectra of complexes **1** and **2** recorded in positive mode gave a peak at m/z 385 (Figs. S1a and S2a) indicating the presence of complexes as $[M+H]^+$. The ESI-MS spectra of complexes **1** and **2** recorded in H_2O–MeOH mixture in a ratio of 10:1 (Figs. S1b and S2b) also show the formation of similar species (peak at m/z 407 $[M+Na]^+$) which ensures that the complexes do not dissociate under experimental conditions [32].

The Infrared spectra for complex **1** produced a very strong band at 1093 cm^{-1} and was assigned to ν(Cl–O) of perchlorate anion (Figs. S3a). Perchlorate bands at 1145 and 640 cm^{-1} belong to an ionic species; this means that this counter-ion is not involved in the cobalt–ligand coordination [33]. Complex-**2** shows strong band at 1381 cm^{-1} for nitrate anions (Figs. S3b).

3.1.1. Crystal structure

The X-ray crystal structure of $[Co(trien)(phen)](ClO_4)_2Cl$ shows that it consists of $[Co(trien)(phen)]^{3+}$ cations and ClO_4^- and Cl^- anions. An ORTEP diagram along with atom numbering scheme for the complex is shown in (Fig. 1). Selected bond distances and bond angles are given in Table 2. The geometry around cobalt (III) is distorted octahedral as shown by the bond parameters. The Co–N distance ranges from 1.9535(15) to 1.9706(14) Å. The N–Co–N bite angle from phen is 83.64(6) whereas from trien, bite angle ranges from 84.35(6) to 86.53(6) Å. The bite angle stems from both trien phen ligand in this complex is similar to the already reported complexes [34–37]. The oxygen atoms of one of the perchlorate anions are disordered. Also one of the methylene carbons (C_1) of trien ligand is found to be disordered.

3.2. DNA binding and cleavage analysis

3.2.1. Absorption spectroscopic study

Electronic absorption spectra were initially employed to study the binding of cobalt (III) complexes with CT-DNA. The absorption spectra in aqueous buffer media of cobalt (III) complexes in the absence and in the presence of CT DNA are given in (Fig. 2). In the UV region, the complexes presented bands at 225 ($\varepsilon = 8.59 \times 10^4$ M^{-1} cm^{-1}), 272 ($\varepsilon = 4.68 \times 10^4$ M^{-1} cm^{-1}) for **1** and 227 ($\varepsilon = 8.71 \times 10^4$ M^{-1} cm^{-1}), 276 ($\varepsilon = 4.7 \times 10^4$ M^{-1} cm^{-1}) for **2**, which can be attributed to $\pi \rightarrow \pi^*$ transition of the

Table 1
Crystal data and structure refinement for complex **1**.

Empirical formula	$C_{18}H_{26}Cl_3CoN_6O_8$
Formula weight	619.73
T (K)	293(2)
Wavelength (Å)	0.71073
Crystal system	triclinic $P\bar{1}$
Space group	
Unit cell dimensions	
a (Å)	7.79760(10)
b (Å)	10.6584(2)
c (Å)	4.8899(3)
α (°)	96.8320(10)
β (°)	96.1620(10)
γ (°)	98.8860(10)
V (A^3)	1203.95(4)
Z	2
Calculated density (Mg/m^3)	1.710
Absorption coefficient (mm^{-1})	1.104
$F(000)$	636
Crystal size (mm)	0.30 × 0.20 × 0.20
Θ Range for data collection (°)	1.39–34.07
Limiting indices	$-12 \leqslant h \leqslant 1$, $-16 \leqslant k \leqslant 16$, $-23 \leqslant l \leqslant 23$
Reflections collected/unique (R_{int})	35175/9730 (0.0278)
Completeness to θ	34.07° to 98.4%
Absorption correction	semi-empirical from equivalents
Maximum and minimum transmission	0.8094 and 0.7330
Refinement method	full-matrix least-squares on F^2
Data/restraints/parameters	9730/33/390
Goodness-of-fit (GOF) on F^2	1.043
Final R indices [$I > 2\sigma(I)$]	$R_1 = 0.0428$, $wR_2 = 0.1205$
R indices (all data)	$R_1 = 0.0572$, $wR_2 = 0.1364$
Largest difference in peak and hole (e A^{-3})	0.842 and −0.719

Table 2
Selected bond length (Å) and angles (°) for complex e A^{-3}.

1	
Important bond distances	
Co(1)–N(1)	1.9535(15)
Co(1)–N(2)	1.9579(15)
Co(1)–N(3)	1.9619(14)
Co(1)–N(4)	1.9706(14)
Co(1)–N(5)	1.9607(14)
Co(1)–N(6)	1.9560(14)
Important bond angles	
N(1)–Co(1)–N(2)	85.27(6)
N(1)–Co(1)–N(3)	96.07(7)
N(1)–Co(1)–N(4)	179.23(6)
N(1)–Co(1)–N(5)	93.67(7)
N(1)–Co(1)–N(6)	87.69(6)
N(2)–Co(1)–N(3)	86.53(6)
N(2)–Co(1)–N(4)	94.11(6)
N(2)–Co(1)–N(5)	95.57(6)
N(3)–Co(1)–N(4)	84.35(6)
N(5)–Co(1)–N(3)	170.18(6)
N(5)–Co(1)–N(4)	85.93(6)
N(6)–Co(1)–N(2)	172.86(6)
N(6)–Co(1)–N(3)	95.45(6)
N(6)–Co(1)–N(4)	92.92(6)
N(6)–Co(1)–N(5)	83.64(6)

coordinated phenanthroline ligand. The absorption intensity of the complexes increased (hyperchromism) evidently after the addition of DNA, which indicated the interactions between DNA and the complexes. A similar hyperchromism has been observed for the soret bands of certain porphyrins when interacted with DNA but has not yet been clearly explained [38,39]. The hyperchromic effect may also be due to the groove binding interaction between positively charged complexes and the negatively charged phosphate backbone at the periphery of the double helix CT DNA [40]. Structurally, intercalation to DNA may be one of the binding patterns, since the cobalt (III) complexes contains phenanthroline ligands which should provide aromatic moiety extending from the metal center through which overlapping occurs with base pairs of DNA by an groove binding mode [41]. The intrinsic binding constant (K_b), was determined from the following equation:

$$[DNA]/(\epsilon_a - \epsilon_f) = [DNA]/(\epsilon_b - \epsilon_f) + 1/K_b(\epsilon_b - \epsilon_f)$$

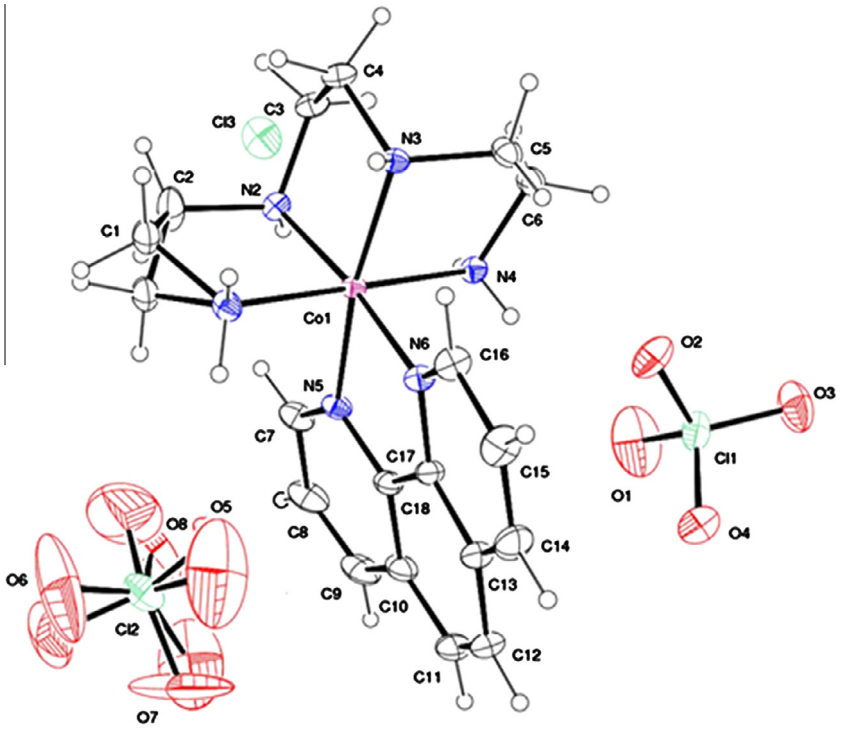

Fig. 1. ORTEP diagram of complex **1** showing the atom labeling scheme (50% probability thermal ellipsoids).

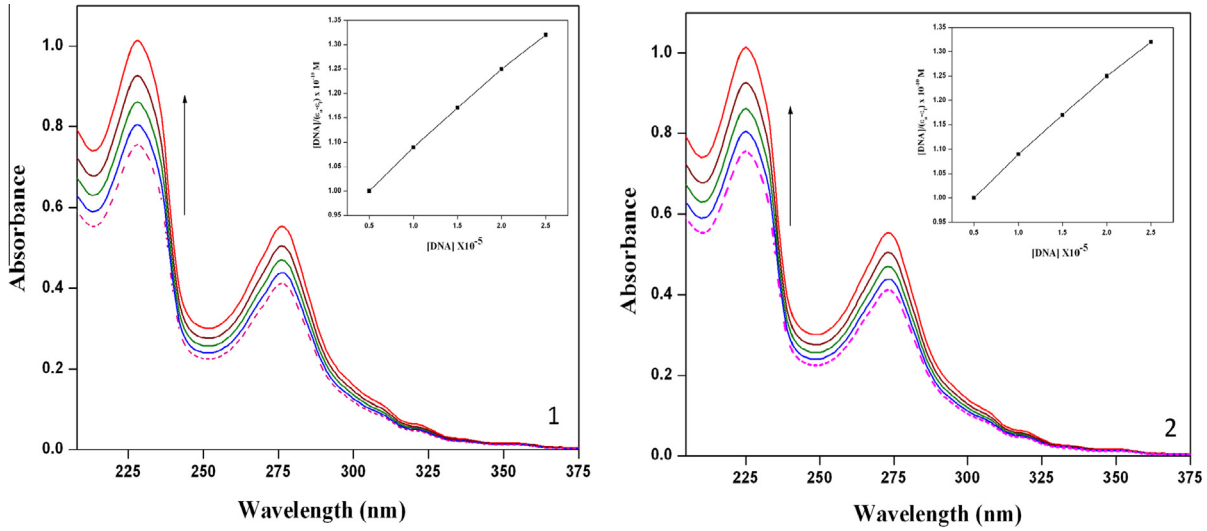

Fig. 2. Electronic spectra of 5.0×10^{-5} M complexes **1** and **2** in the absence (—) and presence (—) of increasing amount of CT DNA at the ratio r = 0.3, 0.5, 0.7, 1.0. Arrow (↑) shows the absorbance changes upon increasing DNA concentration. Inset: linear plot for the calculation of the intrinsic DNA binding constant K_b.

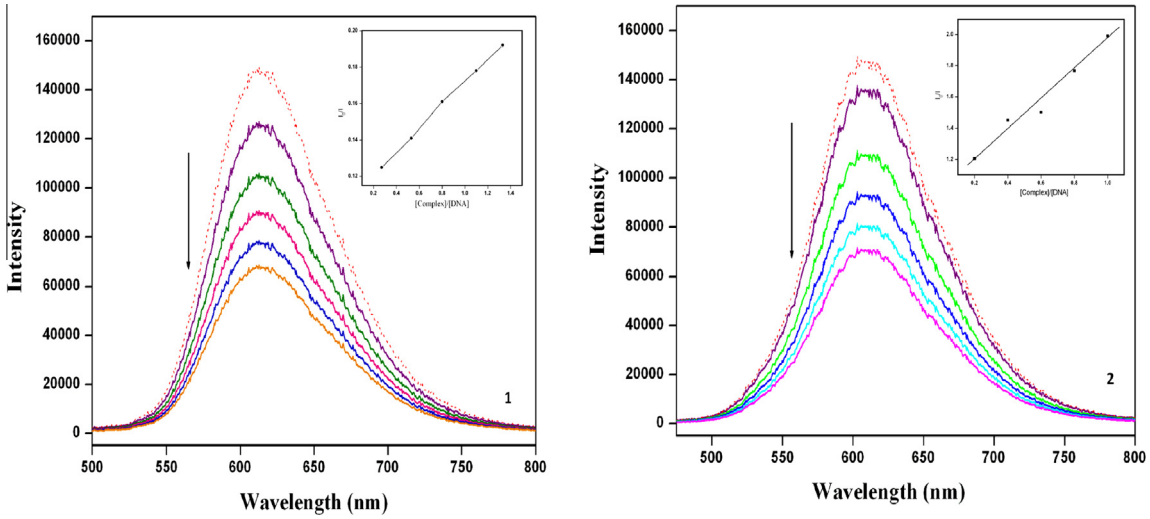

Fig. 3. Emission spectra of EB bound to DNA in the absence (—) and the presence (—) of complexes **1** and **2**, [EB] = 40 μM, [DNA] = 40 μM, [Complex] = (0–50 μM). Arrow (↓) shows the intensity changes upon increasing the concentration of the complex. Inset: Stern–Volmer quenching curves.

The extinction coefficient (ε_a) was obtained by calculating A_{obsd}/[Co]. The terms ε_f and ε_b correspond to the extinction coefficients of free (unbound) and fully bound complexes respectively. A plot of [DNA]/($\varepsilon_a - \varepsilon_f$) versus [DNA] will give a slope $1/(\varepsilon_b - \varepsilon_f)$ and an intercept $1/K_b$ ($\varepsilon_b - \varepsilon_f$). K_b is the ratio of the slope and the intercept [42]. The intrinsic binding constant (K_b) for the association of the complexes with CT DNA (inset of Fig. 2) using the absorption at 272 nm **1** and 276 nm **2** was determined as 8.4761×10^3 **(1)** and 8.3457×10^3 **(2)**. The K_b value is three order of magnitude lower than that observed for classical intercalators such as ethidum bromide (K_b,1.4×10^6 M^{-1}) in 25 mM Tris–HCl/40 mM NaCl buffer, (pH 7.9) [43]. This indicates the complexes have a very low binding affinity to DNA.

3.2.2. Fluorescence binding study

Competitive binding studies using DNA with bound ethidium bromide (EtBr) was carried out for the complexes **1** and **2**. The extent of fluorescence quenching of ethidium bromide (EB) by competitive displacement from DNA is a measure of the strength of interaction between the second molecule and DNA. The results in (Fig. 3) showed that the fluorescence intensity of CT-DNA-EB decreased remarkably with the addition of cobalt complexes, which indicated that the complexes can bind to DNA and replace EB from the CT-DNA-EB system [44]. The above data was analyzed by means of the Stern–Volmer equation [45]. The quenching plots (inset of Fig. 3) illustrates that the fluorescence quenching of EB bound to DNA by the complexes are in linear agreement with the Stern–Volmer relationship, which corroborates that the complexes bind to DNA. In the plot of I_o/I versus [complex]/[DNA], K_{sq} value for the complexes are 0.043 **(1)** and 0.044 **(2)**. The apparent binding constant (K_{app}) is estimated as 0.52×10^5 M^{-1} **(1)** and 0.54×10^5 **(2)** M^{-1} using the equation [46] K_{EB}[EB] = K_{app}[complex], where the complex concentration was the value at a 50% reduction of fluorescence intensity of EB and K_{EB} is 1.0×10^7 $M^{-1}$and [EB] was taken as 40 μM. The difference in the K_{app} value of the complexes compared to K_{EB} value suggests that the complexes are not good interclators as EB.

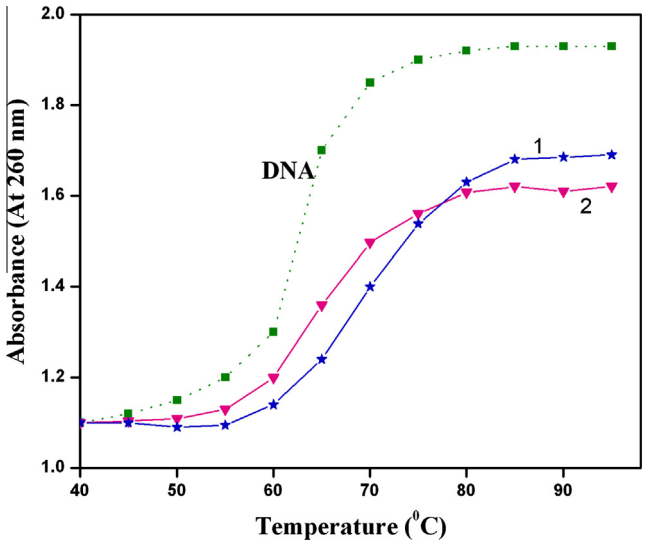

Fig. 4. Thermal denaturation profiles of CT DNA (140 μM) alone and in the presence of complexes **1** and **2** (40 μM) in 5 mM phosphate buffer (pH, 6.85).

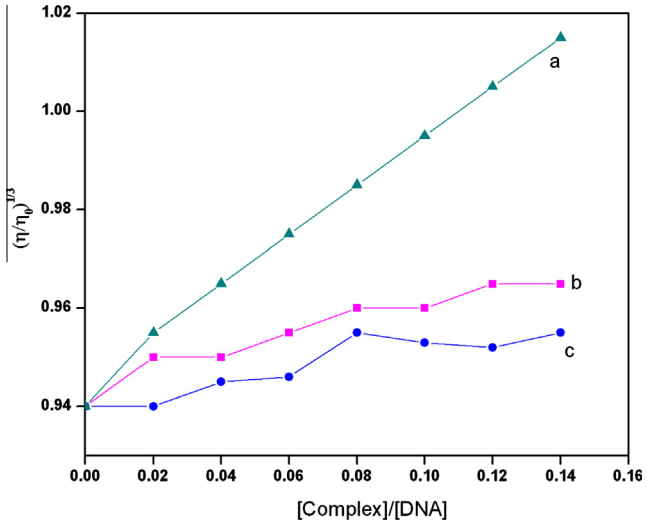

Fig. 5. Effects of increasing amounts of complexes on the relative viscosities of CT DNA at 25 °C: (a) EtBr, (b) complex **1**, (c) complex **2**.

3.2.3. Thermal denaturation study

The DNA melting experiments were carried out to distinguish the different binding modes. The interaction of small molecules with double-helical DNA may increase or decrease the melting temperature Tm, which is defined as the temperature where half of the total base pair gets non-bonded, is a valuable parameter. We have observed a small change in the DNA melting temperature (ΔT_m) on addition of the complexes to CT DNA. The thermal denaturation profile of DNA in the absence and presence of **1** and **2** was provided in (Fig. 4). The low ΔT_m value suggests primarily groove binding of the complexes to CT DNA stabilizing the DNA double helix structure [47].

3.2.4. Viscosity measurement

Mode of interaction between the metal complexes and DNA was clarified by viscosity measurements. A classical intercalation mode demands that the DNA helix lengthens as base pairs are separated to accommodate the bound ligand, leading to the increase of DNA viscosity. In contrast, a partial non-classical intercalation of ligand could bend (or kink) the DNA helix, reduce its effective length and concomitantly its viscosity [24]. Effect of the complexes on the viscosity of rod like DNA is shown in the (Fig. 5). The viscosity of DNA is slightly increased with the increase of the concentration of the complexes **1** and **2**, in contrast to that of proven DNA intercalator EtBr (=ethidium bromide). Based on the viscosity results, it was observed that these complexes bind with DNA through groove binding [48], result from DNA melting experiment further supported the above result.

3.2.5. Cyclic voltammetry studies

The cyclic voltammetric (CV) response for complexes **1** and **2** in Tris–HCl buffer (pH 7.28) in the presence and absence of CT DNA is shown in (Fig. 6). In the forward scan, a single cathodic peak was observed, which corresponds to the reduction of complexes. In the reverse scan, no anodic peak was observed, which indicates that the process is irreversible. When CT-DNA is added to a solution of complexes, marked decrease in the peak current and potential values were observed. The cyclic voltammetric behavior was not affected by the addition of very large excess of DNA, indicating that the decrease of peak current of complexes after the addition of DNA due to the binding of $[Co(trien)(phen)]^{3+}$ complex to the DNA [49]. When the concentration of DNA increased the changes in peak current and potential become slow. This reveals that the complexes were interact with CT-DNA.

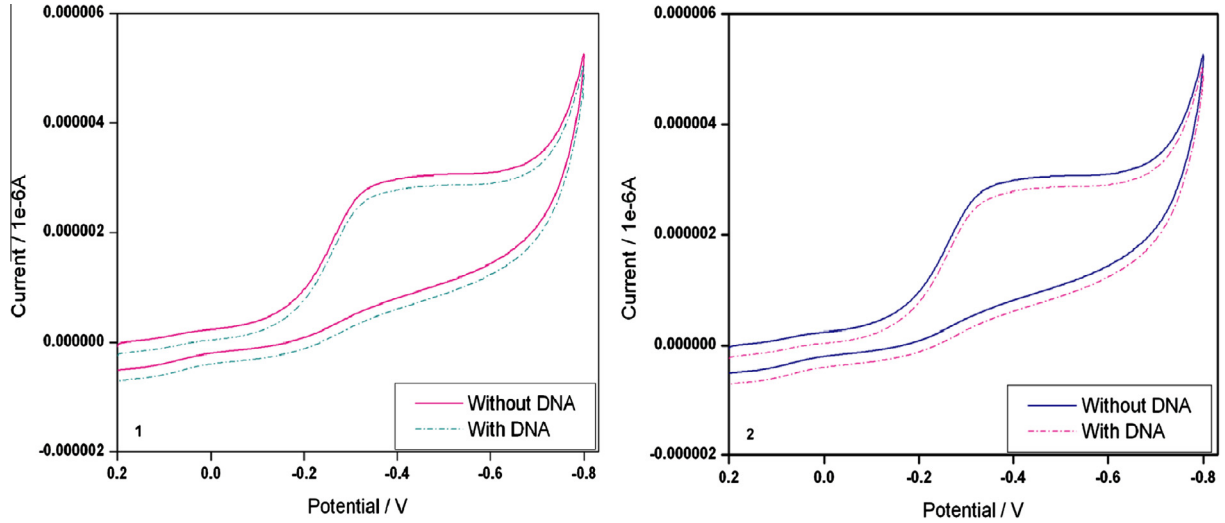

Fig. 6. Cyclic voltammogram of 0.5 mM complexes **1** and **2** in the absence (—) and presence (—) of 2.5 mM DNA.

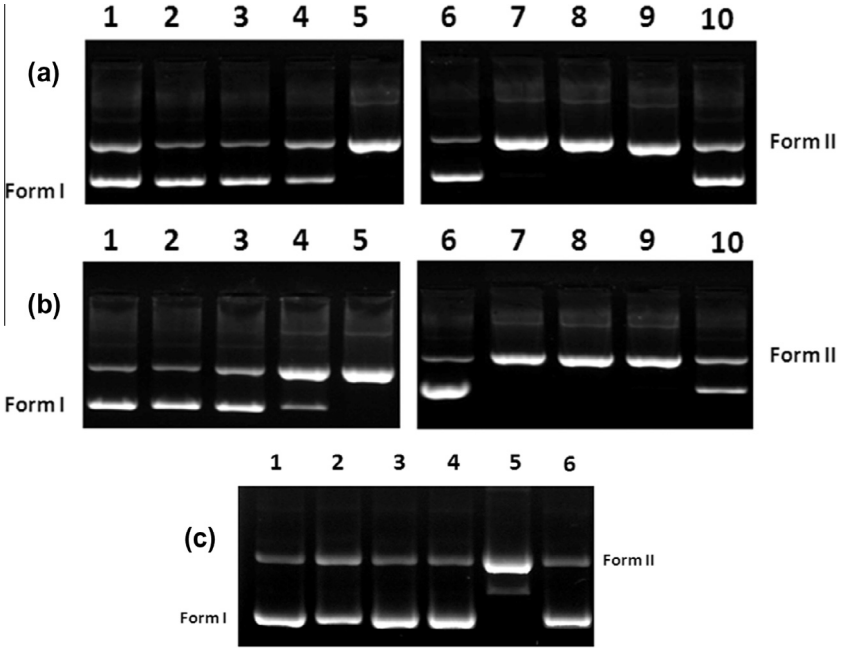

Fig. 7. Cleavage of supercoiled pBR322 DNA by complexes **1** and **2** at different concentrations in the presence of ascorbic acid (H_2A) in 5 mM Tris HCl/50 mM NaCl buffer (pH7.4) at 310 K. (a) Lane 1, DNA control; Lane 2, DNA+ **1** (50 μM); Lane 3, DNA+ **1** (100 μM); Lane 4, DNA+ **1** (150 μM); Lane 5, DNA+ **1** (200 μM); Lane 6, DNA+ H_2A (1 mM); Lane 7, DNA + **1** (10 μM)+ H_2A (1 mM); Lane 8, DNA+ 1(20 μM)+ H_2A(1 mM); Lane 9, DNA+ **1** (30 μM)+ H_2A (1 mM); Lane 10, DNA+ **1** (30 μM)+ H_2A (1 mM)+ DMSO (25 mM); (b) Lane 1, DNA control; Lane 2, DNA+ **2** (50 μM); Lane 3, DNA+ **2** (100 μM); Lane 4, DNA+ **2** (150 μM); Lane 5, DNA+ **2** (200 μM); Lane 6, DNA+ H_2A (1 mM); Lane 7, DNA+ **2** (10 μM)+ H_2A (1 mM); Lane 8, DNA+ **2** (20 μM)+ H_2A (1 mM); Lane 9, DNA+ **2** (30 μM)+ H_2A (1 mM); Lane 10, DNA+**2** (30 μM)+ H_2A (1 mM) + DMSO (25 mM); (c) Lane 1, DNA control; Lane 2, DNA + cobalt (II) chloride(1 mM); Lane 3, DNA+ phen (1 mM); Lane 4, DNA+ trien (1 mM); Lane 5, DNA + H_2A + Complex **1**; Lane 6, DNA + H_2-A + DMSO + Complex **1**.

3.3. DNA Cleavage study

The cleavage activity of complexes **1** and **2** have been investigated by gel electrophoresis using super coiled pBR322 DNA in 50 mM Tris–HCl/50 mM NaCl buffer (pH 7.2). All the complexes were found to exhibit nuclease activity (Fig. 7) in the presence of ascorbic acid (H2A) (Lane: 6–10, Fig. 7a and b for **1** and **2** respectively). Control experiments using only ascorbic acid (H2A) failed to show any significant DNA cleavage under similar experimental conditions (lane 6). This proves the catalytic role of **1** and **2** in the oxidative DNA cleavage.

In order to see the role of hydroxyl radical in the cleavage pathway, an experiment was conducted with DMSO, a hydroxyl radical scavenger. The DMSO completely inhibited the cleavage reaction (lane 10, Fig. 7a and b for **1** and **2** respectively). This suggests the involvement of the hydroxyl radical in the cleavage pathway. Attempts were also made to cleave DNA through hydrolysis of phospodiester bond. Hydrolytic cleavage experiments were performed by treating the SC DNA with **1** and **2** in the absence of external agents (Lane: 1–5, Fig. 7a and b for **1** and **2** respectively). 90% conversion of SC DNA to NC form was achieved at 200 μM by **1** and **2** (Fig. 7a and b, Lane 5). To ensure that the cobalt complexes were solely responsible for the hydrolytic cleavage, control experiments were performed (Fig. 7c). No cleavage was observed with CoCl2 (lane 2) and free ligands (phen and trien; lane 3, 4 respectively.) even at a conc. of 1 mM. When SC pBR 322 DNA was incubated with complex **1** at a concentration of 200 μM in the presence of DMSO, a known radical scavenger, only slight inhibition of DNA cleavage was observed (lane 5, 6 for **1** respectively)

3.4. Antimicrobial screening

The complexes were found to reveal considerable activity against Gram +ve, Gram −ve bacteria and fungi. The results of the antimicrobial activities are summarized in Table 3. The complexes showed greater extent of inhibition to the growth of bacteria. This may be due to the possible mode of increased toxicity of the cobalt complexes. Chelation considerably reduces the polarity of the metal ion because of partial sharing of its positive charge with donor groups and possible π-electron delocalization over the whole chelate ring. Such a chelation could enhance the lipophilic character of the central metal atom, which subsequently favours it permeation through lipid layers of cell membrane and blocking the metal binding sides on enzymes of microorganism. Either the variation in the effectiveness of different compound against different organisms depends on the impermeability of the cells of the microbes or differences in Ribosome's of microbial cells.

Table 3
Antimicrobial activity of complexes **1** and **2**.

Name of the test organism	Complex **1**	Complex **2**
Gram +ve (SD ± mm)		
Staphylococcus aureus	11 ± 0.11	12 ± 0.22
Micrococcus luteus	6 ± 0.31	–
Bacillus cereus	–	–
Gram –ve (SD ± mm)		
Escherichia coli	7 ± 1.3	7 ± 0.14
Klebsiella pneumoniae	8 ± 0.21	9 ± 0.10
Pseudomonas aeruginosa	8 ± 0.34	7 ± 0.21
Fungi		
Aspergillus niger	9 ± 0.12	10 ± 0.10
Aspergillus flaves	–	–
Candida albicans	18 ± 0.13	23 ± 0.41

Ability of the complexes to kill microbes was tested by formation of microbial inhibitory zones on the petri plates containing paper discs soaked in the complex solutions. Inhibitory zones in diameter were calculated on three different petri plates and mean ± SEM are mentioned in the table.

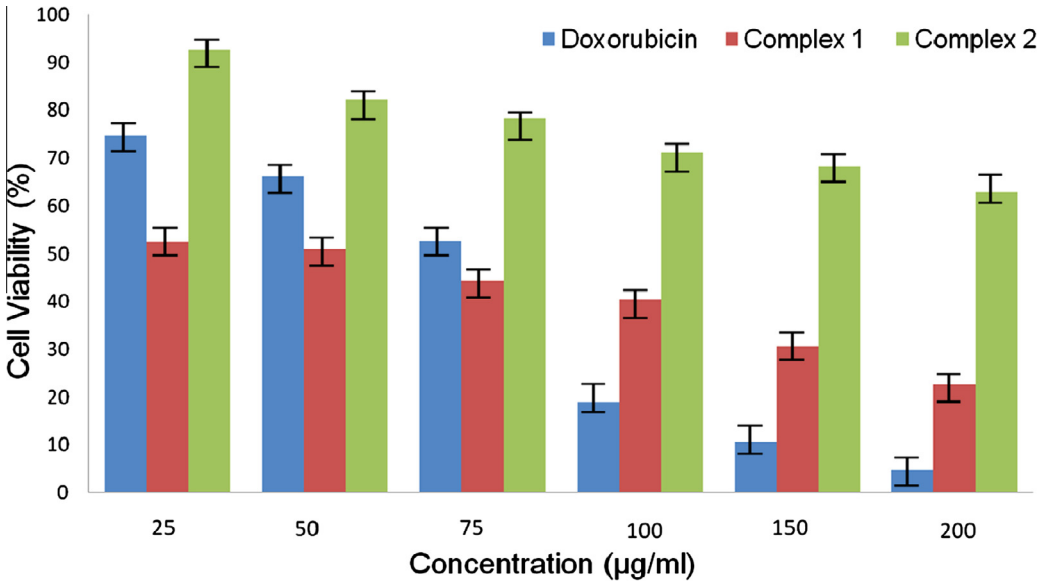

Fig. 8. Cell viability of HepG2 cells after treatment with complexes **1** and **2** at different concentration at 24 h.

Fig. 9. DNA fragmentation. L-1: 1 Kb DNA ladder; L-2: Untreated DNA; L-3: complex **1** treated DNA; L-4: complex **2** treated DNA.

3.5. MTT assay

The cytotoxicity of the complexes to be used as chemotherapeutic agents was studied using MTT assay. The ability of the complexes on HepG2 cells was tested with or without various concentrations (25–200 µg/ml) of complexes **1** and **2** for 24 h. Cells incubated with different concentration of Doxorubicin served as positive control. After incubation period, MTT assay was carried out to calculate the cell death percentage. For each concentration of the complexes cells were incubated in triplicate. The (Fig. 8) clearly illustrates that there is a clear decrease in the live cells number in the cells incubated with complexes in a concentration dependent manner. Viability of cells incubated without any compound was considered as 100% and the percentage of live cells incubated with compounds is given as relative to the control. The IC_{50} value of the complexes **1** and **2** are 59.89 and 464.6 µgm/ml respectively.

3.6. DNA fragmentation

Chromosomal DNA fragmentation is one of the hallmarks of the lethal stages of apoptosis, DNA is initially cleaved into small apoptotic fragments. These DNA fragment 'ladder' is indicative of apoptosis (or programmed cell death) that occurs in the cells in response to the metal based drug. Cultures treated with cobalt complexes demonstrated DNA degradation but did not produce a specific fragmentation pattern at this concentration (Fig. 9). DNA fragment 'ladder' pattern but extensive non-specific DNA fragmentation is visible. From this it is possible to conclude that complexes **1** and **2** activates mammalian cell death by apoptosis and that the other drugs induce non-specific cleavage of DNA possibly due to the nuclease-like activity of the phen ligand.

4. Conclusion

We described here two cobalt (III) complexes. The single crystal structure of complex **1** showed distorted octahedral geometry. Further characterization of the complexes were achieved through physico-chemical and spectroscopic methods. These cobalt (III) complexes attached to DNA by groove binding and exert better anti-microbial and anti-nucleic biological property, however Complex **1** showed higher IC_{50}, suggesting its potential role in medicine as antiseptic and anticancer agents.

Acknowledgements

We are grateful to the IIT Madras, for providing instrumental facilities such as IR spectra, UV–Visible Absorption spectra, Emission spectra and single crystal XRD.

Appendix A. Supplementary material

CCDC 922741 contains the supplementary crystallographic data for **1**. These data can be obtained free of charge from The Cambridge Crystallographic Data Centre via www.ccdc.cam.ac.uk/data_request/cif. Supplementary data associated with this article can be found, in the online version, at http://dx.doi.org/10.1016/j.ica.2014.03.015.

References

[1] A.M. Pyle, E.C. Long, J.K. Barton, J. Am. Chem. Soc. 111 (1989) 4520.
[2] A. Sitlani, E.C. Long, A.M. Pyle, J.K. Barton, J. Am. Chem. Soc. 114 (1992) 2303.
[3] K. Ghosh, V. Mohan, P. Kumar, U.P. Singh, Polyhedron 49 (2013) 167.
[4] Y.-M. Song, X.-L. Lu, M.-L. Yang, X.-R. Zheng, Transition Met. Chem. 30 (2005) 499.
[5] R.S. Kumar, S. Arunachalam, Polyhedron 26 (2007) 3255.
[6] R.S. Kumar, S. Arunachalam, Eur. J. Med. Chem. 44 (2009) 1878.
[7] J.A. Cowan, Curr. Opin. Chem. Biol. 5 (2001) 634.
[8] S. Mathur, S. Tabassum, Cent. Eur. J. Chem. 4 (2006) 502.
[9] J.K. Barton, Science 233 (1986) 727.
[10] M. Carter, M. Rodriguez, A.J. Bard, J. Am. Chem. Soc. 111 (1989) 8901.
[11] X.L. Wang, H. Chao, H. Li, X.L. Hong, Y.J. Liu, L.F. Tan, L.N. JiJ, Inborn. Biochem. 98 (2004) 1143.
[12] H. Shimakoshi, T. Kaieda, T. Matsuo, H. Sato, Y. Hisaeda, Tetrahedron Lett. 44 (2003) 5197.
[13] V.G. Vaidyanathan, B.U. Nair, J. Inorg. Biochem. 94 (2003) 121.
[14] Q.L. Zhang, J.H. Liu, X.Z. Ren, H. Xu, Y. Huang, J.Z. Liu, L.N. Ji, J. Inorg. Biochem. 95 (2003) 194.
[15] P. Nagababu, D.A. Kumar, K.L. Reddy, K.A. Kumar, Md.B. Mustafa, M. Shilpa, S. Satyanarayana, Met-Based Drugs (2008) 1.
[16] A. Klanovica, Z. Travnicek, I. Popa, M. Cajan, K. Dolezal, Polyhedron 25 (2006) 1421.
[17] T.W. Failoes, T.W. Hambley, Dalton Trans. (2006) 1895.
[18] A.M. Sargeson, G.H. Searle, Inorg. Chem. 4 (1965) 45.
[19] J. Marmur, J. Mol. Biol. 3 (1961) 208.
[20] M.E. Reichman, S.A. Rice, C.A. Thomas, P. Doty, J. Am. Chem. Soc. 76 (1954) 3047.
[21] W.D. Wilson, F.A. Tanious, M. Fernandez-saiz, C.T. Rigl, Methods in molecular biology, in: K.R. Fox (Ed.), Humana, Clifton, Nj, 1997.
[22] B.J. Hathaway, A.A.G. Tomlinson, Coord. Chem. 5 (1970) 1.
[23] G. Cohen, H. Eisenberg, Biopolymers 8 (1969) 45.
[24] S. Satyanarayana, J.C. Dabrowiak, J.B. Chaires, Biochemistry 32 (1993) 2573.
[25] J.Y. Zhang, X.Y. Wang, C. Tu, J. Lin, J. Ding, L.P. Lin, Z.M. Wang, C. He, C.H. Yan, X.Z. You, Z.J. Guo, J. Med. Chem. 46 (2003) 3502.
[26] Bruker, APEX2 and SAINT-Plus (version 7.06a). Bruker AXS Inc., 2004
[27] Bruker, SADABS, Bruker AXS Inc., Madison, Wisconsin, USA, 1999.
[28] A. Altormare, G. Gascarano, C. Giacovazzo, A. Guagliardi, J. Appl. Crystallogr. 26 (1993) 343.
[29] G.M. Sheldrick, Acta Crystallogr., Sect. A 64 (2008) 112.
[30] W.J. Geary, Coord. Chem. Rev. 7 (1971) 81.
[31] A. Syamal, P.K. Mandal, Transition Met. Chem. 4 (1979) 348.
[32] P.R. Reddy, A. Shilpa, N. Raju, P. Raghaviah, J. Inorg. Biochem. 105 (2011) 1603.
[33] M.R. Rosenthal, J. Chem. Educ. 50 (1973) 331.
[34] R.P. Sharma, A. Singh, P. Brandao, V. Felix, P. Venugopal, Polyhedron 30 (2011) 2759.
[35] B. Huiye, X. Mingchen, T. Xianzeng, L. Nian Ji, Polyhedron 13 (14) (1994) 2185.
[36] O. Andac, Z. Yolcu, O. Buykgungor, Acta Crystallogr., Sect. E 66 (2010) M46.
[37] N. Azuma, T. Ozawa, Polyhedron 12 (19) (1993) 2291.
[38] R.F. Pasternack, E.J. Gibbs, J.J. Villafranca, Biochemistry 22 (1983) 2406.
[39] C.L. Liu, J.Y. Zhou, Q.X. Li, l.J. Wang, Z.R. Lia, H.B. Xu, J. Inorg. Biochem. 75 (1999) 233.
[40] R. Senthil Kumar, S. Arunachalam, V.S. Periasamy, C.P. Preethy, A. Riyasdeen, M.A. Akbarsha, Polyhedron 27 (2008) 1111.
[41] Z.H. Xu, F.J. Chen, P.X. Xi, X.H. Liu, Z.Z. Zeng, J. Photochem. Photobiol. A. Chem. 196 (2008) 77.
[42] A.M. Pyle, J.P. Rehmann, R. Meshoyrer, C.V. Kumar, N.J. Turro, J.K. Barton, J. Am. Chem. Soc. 111 (1989) 3051.
[43] W.D. Wilson, L. Ratmeyer, M. Zhao, L. Strekowski, D. Boykin, Biochemistry 32 (1993) 4098.
[44] R. Senthil Kumar, S. Arunachalam, V.S. Periasamy, C.P. Preethy, A. Riyasdeen, M.A. Akbarsha, J. Inorg. Biochem. 103 (2009) 117.
[45] J.R. Lakowicz, G. Webber, Biochemistry 12 (1973) 4161.
[46] M. Lee, A.L. Rhodes, M.D. Wyatt, S. Forrow, J.A. Hartley, Biochemistry 32 (1993).
[47] G.L. Eichhorn, Y.A. Shin, J. Am. Chem. Soc. 90 (1968) 7323.
[48] L.S. Kumar, H.D. Revanasldappa, J. Coord. Chem. 64 (2011) 699.
[49] M.C. Prabahkara, H.S.B. Naik, Biometals 21 (2008) 675.